

# Uncovering thermodynamic origin of counterflow and coflow instabilities in miscible binary superfluids

Yu-Ping An,<sup>1,2,\*</sup> Blaise Goutéraux,<sup>3,†</sup> and Li Li<sup>1,2,4,‡</sup>

<sup>1</sup>*CAS Key Laboratory of Theoretical Physics, Institute of Theoretical Physics, Chinese Academy of Sciences, Beijing 100190, China*

<sup>2</sup>*School of Physical Sciences, University of Chinese Academy of Sciences, Beijing 100049, China*

<sup>3</sup>*CPHT, CNRS, École polytechnique, Institut Polytechnique de Paris, 91120 Palaiseau, France*

<sup>4</sup>*School of Fundamental Physics and Mathematical Sciences, Hangzhou Institute for Advanced Study, University of Chinese Academy of Sciences, Hangzhou 310024, China*

In this paper, we explore instabilities in binary superfluids with a nonvanishing relative superflow, particularly focusing on counterflow and coflow instabilities. We extend recent results on the thermodynamic origin of finite superflow instabilities in single-component superfluids to binary systems and derive a criterion for the onset of instability through a hydrodynamic analysis. To verify this result, we utilize both the Gross-Pitaevskii equation (GPE) for weakly interacting Bose-Einstein condensates (BEC) and a holographic binary superfluid model, which naturally incorporates strong coupling, finite temperature, and dissipation. We find that the counterflow and coflow instabilities in binary superfluids are all essentially thermodynamic. Except the one due to order competing via global thermodynamic instability, the others are caused by an eigenvalue of the free energy Hessian diverging and changing sign. We also observe that the critical velocities of these instabilities follow a general scaling law related to the interaction strength between superfluid components. The nonlinear stages of the instabilities are also studied by full time evolution, where vortex dynamics is found to play a significant role, resulting in the reduction of superfluid velocity back to a stable phase.

## I. INTRODUCTION

In both classical fluid systems and quantum superfluids with nonzero velocity, instabilities, such as the Kelvin-Helmholtz instability [1–7], and the two-stream instability [8–15], appear very generally. Such instabilities typically de-

velop into turbulence in nonlinear stage. Understanding the origin and the final fate of these instabilities is crucial to understanding turbulence. Binary superfluids are the most suitable platform to study these instabilities since there is no friction between the two components and one can study equilibrium states with nonzero relative velocity. Such an instability in miscible binary superfluids is often called counterflow insta-

---

\* anyuping@itp.ac.cn

† blaise.gouteraux@polytechnique.edu

‡ liliphy@itp.ac.cn

bility. The counterflow instability of weakly interacting Bose-Einstein condensates (BECs) has been extensively studied [8–11]. However, these studies mostly rely on Gross-Pitaevskii equation (GPE), which is only valid in weak coupling limit, zero temperature, and does not include dissipation.

On the other hand, Gauge-Gravity duality, also known as holography or AdS/CFT (Anti-de Sitter/Conformal Field Theory), has been widely used to study strongly-correlated condensed matter systems without quasiparticles (see [16, 17] for comprehensive reviews). This method connects a pure classical gravity theory to a strong coupling quantum field theory without dynamical gravity on the boundary of the spacetime. Finite temperature, finite density states are modeled by a charged black hole in the bulk. Therefore, in order to study instabilities in binary superfluids, in this work we go beyond the regime of validity of GPE by employing a holographic binary superfluid model, which is intrinsically in the strong coupling limit, and naturally incorporates finite temperature and dissipation. In previous works by some of us [18, 19], we explored dynamical interface instability of strongly interacting binary superfluids. This kind of instability occurs at the interface of immiscible binary superfluids with nonzero superfluid velocity, corresponding to Kelvin-Helmholtz instability. In this work, we focus on instabilities in miscible binary superfluids.

More recently, one of us argued that the dy-

namical instability under linear perturbations of interacting systems in the hydrodynamic regime generally follows from local thermodynamic instability together with positivity of entropy production [20–22]. In particular, the Landau instability in single component superfluids was shown to be essentially thermodynamic. In this work, we extend this result to binary superfluids. By resorting to hydrodynamics of homogeneous binary superfluids, we determine the criterion for thermodynamic instability. To verify this criterion, we analyse both the weakly interacting GPE, and the strongly interacting holographic model. We find that instabilities in both models are essentially thermodynamic.

For GPE, the critical velocity for counterflow instability has already been known for some time [8–11]. In this work we show that the critical instability is correctly predicted by the criterion for thermodynamic instability. For the holographic model, by analysing the spectrum of quasinormal modes (QNMs) on top of stationary states in this model, we identify various instabilities and their critical velocities. Beside the usual counterflow instability, we also find a coflow instability in the holographic model, when the two components flow with the same velocity in the same direction. These instabilities are also identified to be thermodynamic by the same criterion. Interestingly, beyond the criterion from hydrodynamic analysis, there is a global thermodynamic instability due to order competing.

Further, both in GPE and in the holographic

model, we find that the critical velocities of these instabilities present a general scaling law with respect to interaction strength between the two components.

Finally, by using a full nonlinear time evolution scheme, we find that at the endpoint of the instability the superfluid velocity is lowered back to a stable value through vortex formation and annihilation.

This paper is organized as follows. In section II, we present the theory of homogeneous binary superfluids and establish the instability criterion, see equation (17) below. In section III, we study the counterflow instability with GPE and check its onset is predicted by (17). In section IV, we turn to holographic binary superfluids, study their linear instabilities and match to the criterion (17), and determine their nonlinear time evolution. We discuss the universal scaling law of the critical velocity in section V and finish with some conclusions VI. Finally, more details and discussions appear in the appendices.

## II. HYDRODYNAMICS OF HOMOGENEOUS BINARY SUPERFLUIDS

In this section, we extend the formulation in [20–22] to binary superfluids for which there can be in general two conserved  $U(1)$  charges.

Then the conservation equations read <sup>1</sup>

$$\begin{aligned} \partial_t \epsilon + \partial_i j_\epsilon^i &= 0, & \partial_t g^i + \partial_i \tau^{ji} &= 0, \\ \partial_t n_I + \partial_i j_I^i &= 0, & (I = 1, 2), \end{aligned} \quad (1)$$

where  $\epsilon$ ,  $g^i$  and  $n_I$  are the energy, momentum and charge densities,  $j_\epsilon^i$  and  $j_I^i$  are the energy and charge currents, and  $\tau^{ji}$  is the spatial stress tensor. The former two equations follow from invariance under time and space translations, respectively, and the last one is from  $U(1)$  global transformations. Denoting  $\mathbf{v}^n$  to be the normal fluid velocity and  $\mathbf{v}_I^s$  the superfluid velocities, one has the Josephson relations:

$$\partial_t \varphi_I + \mathbf{v}^n \cdot \partial \varphi_I + \mu_I = 0, \quad (2)$$

where  $\mu_I$  is the chemical potential (including possible derivative corrections, see below) and  $\varphi_I$  the Goldstone field for the  $I$ -th superfluid component. The latter is closely related to the superfluid velocity,  $\mathbf{v}_I^s = \nabla \varphi_I$ .

In this paper we work in the grand-canonical ensemble where the thermodynamic variables are the temperature  $T$ , the chemical potential  $\mu$  and the norm of the superfluid velocities  $v_I^s = |\mathbf{v}_I^s|$ . The first law of thermodynamics reads

$$\begin{aligned} d\epsilon &= T ds + \mu^I dn_I + \mathbf{v}^n dg \\ &+ \mathbf{h}^I d\mathbf{v}_I^s + Nd(\mathbf{v}_1^s \cdot \mathbf{v}_2^s), \end{aligned} \quad (3)$$

---

<sup>1</sup> While we find it convenient to write the conservation equations and constitutive relations for the spatial fluxes non-covariantly, for the purposes of this work we always have in mind systems ultimately invariant under Galilean or Lorentz boost, which set  $g^i = j_1^i + j_2^i$  and  $j_\epsilon^i = j_\epsilon^i$ , respectively.

where  $s$  is the entropy density,  $\mathbf{v}^n$  is the normal fluid velocity, and  $\mathbf{h}_I = n_I^s(\mathbf{v}_I^s - \mathbf{v}^n)$  with  $n_I^s$  being the superfluid charge density ( $I$  is not summed here). In contrast to the single component case [20], there is an additional cross term which accounts for the energy change due to relative motion between the two components of superfluids.<sup>2</sup> By introducing  $\bar{\mathbf{h}}_I = \mathbf{h}_I + N\sigma^{IJ}\mathbf{v}_J^s$  with  $\sigma^{IJ} = \begin{pmatrix} 0 & 1 \\ 1 & 0 \end{pmatrix}$ , this cross term can be absorbed and one has

$$d\epsilon = Tds + \mu^I dn_I + \mathbf{v}^n d\mathbf{g} + \bar{\mathbf{h}}^I d\mathbf{v}_I^s. \quad (4)$$

Unless otherwise stated, repeated capital Latin flavour indices  $I, J, \dots$  are summed over, just like the usual small case Latin spatial indices  $i, j, \dots$  (*i.e.* the Einstein summation convention).

We now consider dissipative corrections to the idea order constitutive relations, for which we shall use tilde to label dissipative corrections. Then from positivity of entropy production

$$T\partial_t s + T\partial_i(sv^{ni} + \tilde{j}_s^i/T) \equiv \Delta \geq 0, \quad (5)$$

we can obtain the constitutive relations for the currents in equilibrium state compatible with parity and time-reversal invariance:

$$\begin{aligned} j_I^i &= n_I v^{ni} + \bar{h}_I^i + \tilde{j}_I^i, \\ j_\epsilon^i &= (\epsilon + p)v^{ni} + \partial_t \varphi^I \bar{h}_I^i + \tilde{j}_\epsilon^i, \\ \tau^{ji} &= p\delta^{ij} + v^{ni}g^j + \bar{h}_I^j v_s^{Ii} + \tilde{\tau}^{ji}, \end{aligned} \quad (6)$$

<sup>2</sup> In principle in absence of boost invariance there is a relative coefficient between  $\mathbf{v}_I^s$  and  $\mathbf{v}^n$  in  $\mathbf{h}_I$  [23]. As it plays no role in our analysis, we have set it to unity.

where  $p = -\epsilon + sT + n_I\mu_I + v^{ni}g_i$ , and tilded quantities are first-order derivative corrections. To first order, the entropy production is given by

$$\Delta = -\tilde{j}_s^i \partial_i T/T - \tilde{j}_I^i \partial_i \mu^I - \tilde{\tau}^{ji} \partial_i v_j^n - \tilde{\mu}^I \partial_i \bar{h}_I^j, \quad (7)$$

where  $\tilde{\mu}^I$  are derivative corrections in the Josephson equations.

Next, we turn to the dynamical instability from hydrodynamics. One can linearize the equations of motion (EoMs) around equilibrium state by perturbing the thermodynamic quantities  $O_A = O_{A0} + e^{-i\omega t + i\mathbf{k}\cdot\mathbf{x}}\delta O_A$  and their sources  $s_A = s_{A0} + e^{-i\omega t + i\mathbf{k}\cdot\mathbf{x}}\delta s_A$ , where  $O_A = (s, \mathbf{g}, n_I, \mathbf{v}_I^s)$  and  $s_A = (T, \mathbf{v}^n, \mu_I, \bar{\mathbf{h}}_I)$ . They are related by static susceptibility matrix  $\chi_{AB} = \delta O_A / \delta s_B = \delta^2 F / \delta s_A \delta s_B$ , where  $F = -T \ln Z$  is the thermal free energy. The linearized EoMs in Fourier space would be

$$\begin{aligned} (-i\omega + i\mathbf{k} \cdot \mathbf{v}^n)\delta O_A + M_{AB}(\mathbf{k})\delta s_B &= 0 \\ \Rightarrow (-i\tilde{\omega} + M(\mathbf{k}) \cdot \chi^{-1})\delta O &= 0, \end{aligned} \quad (8)$$

where  $\tilde{\omega} = \omega - \mathbf{k} \cdot \mathbf{v}^n$ . Then the spectrum of collective modes can be obtained by solving  $\det(-i\tilde{\omega} + M \cdot \chi^{-1}) = 0$ . The onset of a dynamical instability occurs when the imaginary part of  $\tilde{\omega}$  becomes positive. This can happen when  $\det(M \cdot \chi^{-1}) = \det(M) / \det(\chi)$  vanishes and changes sign. It can be shown that  $\det(M) > 0$  following [22]. Therefore, an instability can only occur when  $\det(\chi)$  diverges and changes sign. Such instability from the divergence of the susceptibility matrix is obviously thermodynamic.

We now proceed by choosing a frame where  $\mathbf{v}^n = 0$ . This is the case for holographic superfluids in the probe limit, and also for the superfluids modeled by GPE. We are interested in the effects from superfluid velocities, so we keep the temperature fixed from now on. For simplicity, we shall consider the case where the chemical potentials and charge densities are the same for both superfluid components.<sup>3</sup> Then the thermodynamic quantities and sources we need to consider are just  $\{n_I = (n, n), \mathbf{v}_I^s\}$  and  $\{\mu_I = (\mu, \mu), \bar{\mathbf{h}}_I\}$ . In this case, the EoMs are

$$\begin{aligned} \partial_t n + \partial_i(j^i + \tilde{j}^i) &= 0, \\ \partial_t v_I^{s_i} + \partial_i(\mu_I + \tilde{\mu}_I) &= 0. \end{aligned} \quad (9)$$

After considering the Onsager reciprocity and

the positivity of entropy production, the first-order derivative corrections can be parameterized as

$$\begin{aligned} \tilde{j}^i &= \sigma_1 \partial^i \mu + \sigma_2 \frac{v_J^{s_i} v_J^{s_j}}{|v_J^s|^2} \partial_j \mu + \beta v_I^{s_i} \partial_j \bar{h}^{Ij}, \\ \tilde{\mu}_I &= \beta v_I^{s_j} \partial_j \mu + \delta_1 \partial_j \bar{h}_I^j + \delta_2 v_I^{s_i} v_{J_i}^s \partial_j \bar{h}^{Jj}, \end{aligned} \quad (10)$$

where  $(\sigma_1, \sigma_2, \beta, \delta_1, \delta_2)$  are five non-hydrostatic positive parameters.<sup>4</sup>

The case with general superfluid velocities is still very complicated. We focus on the collinear case where  $\mathbf{v}_1^s // \mathbf{v}_2^s // \mathbf{k}$ .<sup>5</sup> For later convenience, we change variables to

$$\begin{aligned} v_+^s &= \frac{v_1^s + v_2^s}{2}, & v_-^s &= \frac{v_1^s - v_2^s}{2}, \\ \bar{h}_+ &= \bar{h}_1 + \bar{h}_2, & \bar{h}_- &= \bar{h}_1 - \bar{h}_2. \end{aligned} \quad (11)$$

By linearizing the EoMs (9) one can find the matrix  $M_{AB}$  to be

$$M = \begin{pmatrix} \sigma k^2 & ik + \beta v_+^s k^2/2 & \beta v_-^s k^2/2 \\ ik + \beta v_+^s k^2/2 & (\delta_1 + \delta_2 (v_+^s)^2) k^2/4 & \delta_2 v_+^s v_-^s k^2/4 \\ \beta v_-^s k^2/2 & \delta_2 v_+^s v_-^s k^2/4 & (\delta_1 + \delta_2 (v_-^s)^2) k^2/4 \end{pmatrix}, \quad (12)$$

with  $\sigma = \sigma_1 + 2\sigma_2$ . In above equation, we have treated  $\bar{h}_I$  as source for the convenience of linearizing EoMs. In practice, it is more con-

venient to treat  $v_I^s$  as source. Let us denote  $(n, v_I^s)^T = \tilde{\chi} \cdot (\mu, \bar{h}_I)^T$  and  $(n, \bar{h}_I)^T = \chi \cdot (\mu, v_I^s)^T$ .

Then we can express  $\tilde{\chi}$  in terms of  $\chi$ :

<sup>3</sup> This is equivalent to setting the imbalance charge density  $n_- = n_1 - n_2$  identically to zero. This can straightforwardly be relaxed if needed.

<sup>4</sup> In principle,  $\tilde{j}^i$  can be different for each component, *i.e.*  $\Delta \tilde{j}^i = \tilde{j}_1^i - \tilde{j}_2^i \neq 0$ . Nevertheless, from (1) one

has  $\partial_i \Delta \tilde{j}^i = 0$  since  $n_1 = n_2$ . On the other hand, only divergence of  $\tilde{j}^i$  appears in the EoMs (9). Therefore,  $\Delta \tilde{j}^i$  has no effects and one can simply take  $\tilde{j}_1^i = \tilde{j}_2^i = \tilde{j}^i$ .

<sup>5</sup> There is no conceptual obstacle generalising to other cases. But the resulting expressions are very lengthy.

$$\tilde{\chi} = \begin{pmatrix} \chi_{nn} + \chi_{n+} \frac{\chi_{n+}\chi_{--} - \chi_{n-}\chi_{-+}}{\chi_{++}\chi_{--} - \chi_{+-}\chi_{-+}} + \chi_{n-} \frac{-\chi_{n+}\chi_{+-} + \chi_{n-}\chi_{++}}{\chi_{++}\chi_{--} - \chi_{+-}\chi_{-+}} & \frac{\chi_{n+}\chi_{--} - \chi_{n-}\chi_{-+}}{\chi_{++}\chi_{--} - \chi_{+-}\chi_{-+}} & \frac{-\chi_{n+}\chi_{+-} + \chi_{n-}\chi_{++}}{\chi_{++}\chi_{--} - \chi_{+-}\chi_{-+}} \\ \frac{\chi_{n+}\chi_{--} - \chi_{n-}\chi_{-+}}{\chi_{++}\chi_{--} - \chi_{+-}\chi_{-+}} & \frac{\chi_{--}}{\chi_{++}\chi_{--} - \chi_{+-}\chi_{-+}} & \frac{-\chi_{+-}}{\chi_{++}\chi_{--} - \chi_{+-}\chi_{-+}} \\ \frac{-\chi_{n+}\chi_{+-} + \chi_{n-}\chi_{++}}{\chi_{++}\chi_{--} - \chi_{+-}\chi_{-+}} & \frac{-\chi_{-+}}{\chi_{++}\chi_{--} - \chi_{+-}\chi_{-+}} & \frac{\chi_{++}}{\chi_{++}\chi_{--} - \chi_{+-}\chi_{-+}} \end{pmatrix}, \quad (13)$$

where  $\chi_{nn} = \partial n / \partial \mu|_{v_I^s}$ ,  $\chi_{nI} = \partial n / \partial v_I^s|_{\mu}$  and  $\chi_{IJ} = \partial \bar{h}_I / \partial v_J^s|_{\mu}$ . We also have  $\chi_{+-} = \chi_{-+}$  from Onsager relation (and also from  $\chi_{AB} \equiv \delta^2 f / \delta s_A \delta s_B$ ) where  $f$  is the free energy density. By solving (8) with (12) and (13), we find two

sound modes and one diffusive mode:

$$\begin{aligned} \omega_{\pm} &= v_{\pm} k + i\Gamma_{\pm} k^2 + \mathcal{O}(k^3), \\ \omega_0 &= -i\Gamma_0 k^2 + \mathcal{O}(k^3), \end{aligned} \quad (14)$$

where

$$\begin{aligned} v_{\pm} &= \frac{-\chi_{n+} \pm \sqrt{\chi_{n+}^2 + \chi_{++}\chi_{nn}}}{\chi_{nn}}, \\ \Gamma_0 &= \frac{(\chi_{++}\chi_{--} - \chi_{+-}^2)(\delta_2(v_-^s)^2 + \delta_1)}{4\chi_{++}}, \end{aligned} \quad (15)$$

$$\begin{aligned} \Gamma_{\pm} &= \frac{1}{4(\chi_{++} - v_{\pm}(4\chi_{n+} + 3v_{\pm}\chi_{nn}))} \\ &(\delta_1(v_{\pm}^2\chi_{nn}(\chi_{++} + \chi_{--}) + (v_{\pm}\chi_{n-} - \chi_{+-})^2 + v_{\pm}\chi_{n+}(2\chi_{--} + v_{\pm}\chi_{n+}) - \chi_{++}\chi_{--}) \\ &+ \delta_2(v_{\pm}^2(v_{\pm}^s)^2(\chi_{n+}^2 + \chi_{++}\chi_{nn}) + (v_{\pm}^s)^2(v_{\pm}^2\chi_{--}\chi_{nn} + (v_{\pm}\chi_{n-} - \chi_{+-})^2 + (2v_{\pm}\chi_{n+} - \chi_{++})\chi_{--}) \\ &+ 2v_{\pm}v_{\pm}^s v_{\pm}^s(\chi_{n-}(v_{\pm}\chi_{n+} - \chi_{++}) + \chi_{+-}(v_{\pm}\chi_{nn} + \chi_{n+}))) + 4\sigma v_{\pm}^2 \\ &+ 4\beta(v_{\pm}^s + v_{\pm}^s)v_{\pm}(v_{\pm}^s(v_{\pm}\chi_{n+} - \chi_{++}) + v_{\pm}^s(v_{\pm}\chi_{n-} - \chi_{+-}))), \end{aligned} \quad (16)$$

with  $\delta_1$ ,  $\delta_2$ ,  $\beta$  and  $\sigma$  positive constants.

The criterion for the onset of instability is given by  $\det(\tilde{\chi}) = -\chi_{nn}/(\chi_{++}\chi_{--} - \chi_{+-}^2)$  diverging and changing sign. It gives

$$\chi_{++}\chi_{--} - \chi_{+-}^2 = 0, \quad (17)$$

at which both the sound and diffusive modes of (14) could begin to develop a positive imaginary frequency, causing perturbations to grow exponentially. One can directly verify that the

criterion (17) is also the same for non-identical binary superfluids for which  $n_1 \neq n_2$ . The calculation is straightforward but lengthier.

For the counterflow case where  $v_{+}^s = 0$  and the coflow case where  $v_{-}^s = 0$ , we have  $\chi_{+-} = 0$ , since  $\chi_{+-} = \delta^2 f((v_{+}^s)^2, (v_{-}^s)^2) / (\delta v_{+}^s \delta v_{-}^s) \sim v_{+}^s v_{-}^s$ . Therefore, in both cases, the criterion for the onset of instability is given by  $\chi_{++} = 0$  or  $\chi_{--} = 0$ . We will see later this is indeed the correct criteria for onset of counterflow and coflow

instabilities in the holographic binary superfluid model. It also explains the counterflow instability found from GPE.

### III. COUNTERFLOW INSTABILITY FROM GPE

The development of quantum turbulence from two counter-propagating superfluids of miscible BECs has been studied using the mean-field GPE [8–11]. In the mean field approximation, the condensate wave functions are described by  $\Psi_J(x, y, t) = \sqrt{n_J^s(x, y, t)}e^{i\theta_J(\mathbf{r}, t)}$  where  $n_J^s$  and  $\theta_J$  are the particle density and phase of the  $J$ -th component of the binary superfluids. The latter is nothing but the Goldstone field  $\varphi_J$  for the  $J$ -th superfluid component. The coupled GPEs are given as (capital Latin indices are not summed here)

$$i\partial_t\Psi_I = \left(-\frac{1}{2m_I}\nabla^2 - \mu_I + g_I|\Psi_I|^2 + g_{IJ}|\Psi_J|^2\right)\Psi_I, \quad (18)$$

( $I, J = 1, 2, \quad I \neq J$ ),

which describes binary superfluids without dissipation and normal fluid component. Here  $m_I$  is the mass of the  $I$ -th component, and  $g_1, g_2$  and  $g_{12}$  are the coupling constants. To obtain stable miscible condensates, we consider the conditions  $g_{12} < \sqrt{g_1 g_2}$  and  $g_I > 0$ .

It was shown that the countersuperflow becomes unstable and quantized vortices are nucleated as the relative velocity exceeds a critical value, leading to isotropic quantum turbulence consisting of two superflows. In contrast to

the Landau instability stemming from thermodynamic instability, it was argued that the counterflow instability is purely an “internal” instability of the isolated system of two superfluids without any influence from the external environment. As a dynamic instability, the physical origin of the counterflow instability observed in the coupled GPEs is still unclear.

Interestingly, we show that the counterflow instability of the two-component BECs via (18) is indeed a thermodynamic instability in the sense  $\det(\tilde{\chi})$  diverges. For the case where there are two  $U(1)$  conserved charges, one can find this also happens when (17) is satisfied. To be more specific, it is given by

$$\chi_{++} = n_+^s + v_-^s \partial_{v_+^s} n_-^s + N = 0. \quad (19)$$

For simplicity, let’s consider the case where  $m_1 = m_2 = m$ ,  $g_1 = g_2 = g$  and  $\mu_1 = \mu_2 = \mu$ . From (18), the superfluid densities for stationary and uniform state can be found to be

$$n_I^s = \frac{g(\mu - \frac{m}{2}(v_I^s)^2) - g_{12}(\mu - \frac{m}{2}(v_J^s)^2)}{g^2 - g_{12}^2}, \quad (20)$$

$I, J = 1, 2, \quad I \neq J,$

with  $n_I^s = |\Psi_I|^2$ . In terms of  $v_+^s$  and  $v_-^s$  of (11), the corresponding densities are

$$n_+^s = \frac{2\mu - m((v_+^s)^2 + (v_-^s)^2)}{g + g_{12}}, \quad (21)$$

$$n_-^s = -\frac{2mv_+^s v_-^s}{g - g_{12}}.$$

We can obtain  $N$  by noting that

$$\chi_{+-} - \chi_{-+} = v_-^s \partial_{v_+^s} N - \frac{4v_+^s v_-^s g_{12}}{g^2 - g_{12}^2} = 0. \quad (22)$$



Therefore, we have  $N = 2(v_+^s)^2 g_{12}/(g^2 - g_{12}^2)$ , which is 0 for  $v_+^s = 0$ , *i.e.* the counterflow case. Then the criterion for the onset of instability is given by

$$\chi_{++}|_{v_+^s=0, v_-^s=v_c} = \frac{2\mu - mv_c^2}{g + g_{12}} - \frac{2mv_c^2}{g - g_{12}} = 0, \quad (23)$$

which gives

$$v_c = \sqrt{(g - g_{12})n_+^s/2m}. \quad (24)$$

This is exactly the critical velocity derived from Bogoliubov–de Gennes analysis [8–11], with  $n_+^s = 2n$ . Therefore, the dynamical counterflow instability found by numerically solving the coupled GPEs is essentially thermodynamic in origin.

#### IV. HOLOGRAPHIC BINARY SUPERFLUIDS

We then move to the gravity description of a two-component superfluid in two spatial dimensions. More details are given in appendix A. The system involves two complex scalar operators  $\hat{\mathcal{O}}_I$  which carry the same charge  $e$  under a global  $U(1)$  symmetry.<sup>6</sup> Below a critical temperature  $T_c$ , the scalar operators develop a nonzero expectation value spontaneously breaking the  $U(1)$  symmetry and driving the system into a superfluid phase. The holographic system in (3+1)-dimensional asymptotically anti-de Sitter

<sup>6</sup> Thus there will be only one conserved density, which is a special limit of the hydrodynamic and GPE analyses of the previous sections.

(AdS) spacetime involves a bulk dynamical  $U(1)$  gauge field  $A_\mu$  and the scalar operators  $\hat{\mathcal{O}}_i$  are mapped to two bulk scalar fields  $(\Psi_1, \Psi_2)$  carrying charge  $e$  under  $A_\mu$ . For definiteness we will choose two identical scalar fields with the potential  $V(\Psi_1, \Psi_2) = m^2(|\Psi_1|^2 + |\Psi_2|^2) + \frac{\nu}{2}|\Psi_1|^2|\Psi_2|^2$  with a mass for  $(\Psi_1, \Psi_2)$  correspond to the dual scalar operators having the scaling dimension  $\Delta = 2$ . The inter-component coupling  $\nu$  characterizes the interaction between two components of superfluids and determines the miscibility of the superfluids [18]. For the homogeneous case with  $\nu > 0$ , only one of the superfluid condensations can develop spontaneously below the critical temperature  $T_c$  (immiscible binary superfluids), while  $\nu < 0$  gives miscible binary superfluids, which is the focus of this work.

At finite temperature, each of the two species contains both superfluid and normal components. This appears to be a rather complicated problem. To avoid these complications, without loss of generality we consider the case where the fluctuations of the temperature and the normal fluid velocity are frozen, and meanwhile, the dynamics of momentum and energy are decoupled from the charge sector. This corresponds to the probe limit in the gravity description for which the back-reaction of matter content to the geometry is neglected. More precisely, the background is given by the Schwarzschild AdS black brane (see Appendix A for details on the bulk action and the metric we use). After solving the bulk EoMs, we can read off all relevant observ-



ables by the standard holographic dictionary, including the temperature  $T$ , the superfluid velocity  $\mathbf{v}_I^s \equiv (v_{Ix}^s, v_{Iy}^s)$  for each superfluid condensation  $\mathcal{O}_I \equiv \langle \hat{\mathcal{O}}_I \rangle$ . The gravity dual thus provides a first-principle description of superfluid dynamics.

The phase-separated binary superfluids have been studied recently in [18, 19, 24] in holography, where rich dynamics were uncovered. Here we are interested in the holographic miscible binary superfluids, which provides a good platform for checking the hydrodynamic framework in Section II. The construction of the stationary configuration for miscible binary superfluids is provided in Appendix B.

### A. Dynamical instability from linear analysis

In this section we study dynamical counterflow and coflow instability in miscible holographic binary superfluids using linear response theory. To do this, we turn on small perturbations  $\sim e^{-i(\omega t - \mathbf{k} \cdot \mathbf{x})}$  on the stationary background, thanks to the translation invariance of the background along the time and spatial directions. Due to the dissipation of the system, the frequency  $\omega$  typically takes a complex value. Dynamical instability is triggered once its imaginary part  $\text{Im}\omega > 0$  at some value of wave number  $\mathbf{k}$ . This is known as the QNM analysis in black

hole physics.<sup>7</sup>

Without loss of generality, we assume that the superfluids move along the  $y$  direction with the velocity  $v_y$ . More precisely, the counterflow case corresponds to  $\mathbf{v}_1^s = -\mathbf{v}_2^s = (0, v_y)$ , and the coflow one has  $\mathbf{v}_1^s = \mathbf{v}_2^s = (0, v_y)$ . Since the instability will typically develop fastest along the flow of the superfluids, we consider the wave vectors parallel to the superfluid velocity, *i.e.*  $\mathbf{k} \cdot \mathbf{x} = ky$ . The full set of linearized EoMs can be found in Appendix D, which results in a generalized eigenvalue problem that can be solved numerically. In Figure 1, we give a representative example for the counterflow instability (upper panel) and the coflow instability (lower panel), where we show the dominant QNMs with respect to the wave number  $k$ . While the spectral patterns are quite different, one finds that a dynamical instability will develop beyond a critical velocity for both counterflow and coflow cases.

The spectrum of QNMs for the case with  $\nu = 0$  and  $v_y = 0$  was studied in [25] where the scalar fields transform as a doublet, *i.e.* a global  $SU(2)$  symmetry. It was found that there exist two kinds of gapless modes. One is the sound mode of the superfluid, and the dispersion relations is linear in the hydrodynamic limit  $\omega_I = \pm(v_s k + \bar{b}k^2) - i\Gamma k^2$  which is classified as the type I Goldstone boson [26] and is due to the spontaneous breaking of  $U(1)$  symmetry. The

<sup>7</sup> Both the hydrodynamic modes and non-hydrodynamic of the boundary systems can be obtained by the QNMs of the dual black hole.

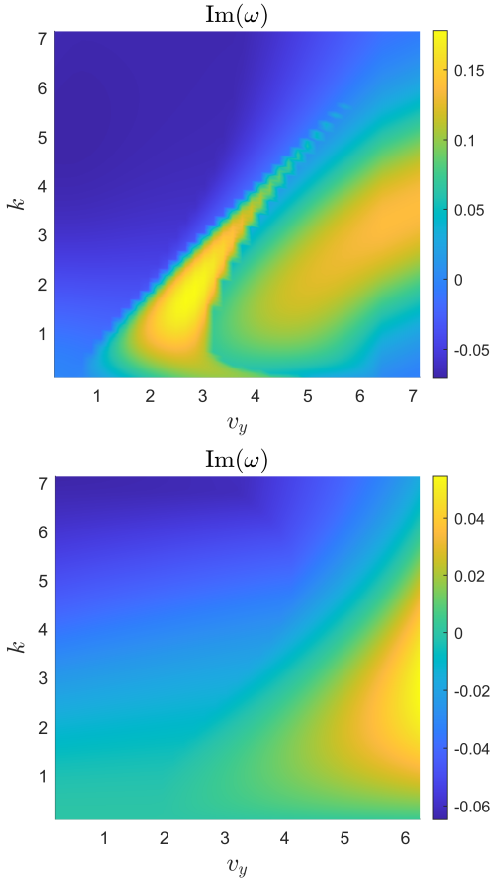


Figure 1. The QNMs spectrum with respect to  $k$  and  $v_y$  for the counterflow case (top) and the coflow cases (bottom). The stationary configuration is dynamical unstable whenever  $\text{Im}\omega_k > 0$ . We have considered holographic miscible binary superfluids at  $T/T_c = 0.677$  and  $\nu = -0.2$ .

other presents quadratic dispersion relation at small  $k$ ,  $\omega_{\text{II}} = \pm bk^2 - ick^2$ , and is classified as the type II Goldstone boson. This mode appears because of spontaneous breaking of the bulk global  $SU(2)$  symmetry. When  $\nu \neq 0$ , the  $SU(2)$  symmetry is explicitly broken. But there is a residual  $U(1) \times U(1)$  symmetry. Therefore, one branch of type II Goldstone boson becomes gapped, while the other branch remains gapless

but becomes a dissipative, quadratic mode. This is clearly shown in Figure 2, from which there are two modes with linear dispersion relation (red line), one mode with quadratic dispersion relation (blue line) and a gapped mode (black line).

$$\begin{aligned}\omega_{\pm} &= \pm v_s k - i\Gamma k^2 + \mathcal{O}(k^3), \\ \omega_0 &= -i\Gamma_0 k^2 + \mathcal{O}(k^3), \\ \omega_{gap} &= -i\Gamma_{gap} + \mathcal{O}(k).\end{aligned}\quad (25)$$

We find that this pattern is true for all parameters of our holographic binary superfluids, as long as  $\nu < 0$ . And this is also consistent with the result of (14) from hydrodynamics of binary miscible superfluids (which does not incorporate the dynamics of the gapped mode).

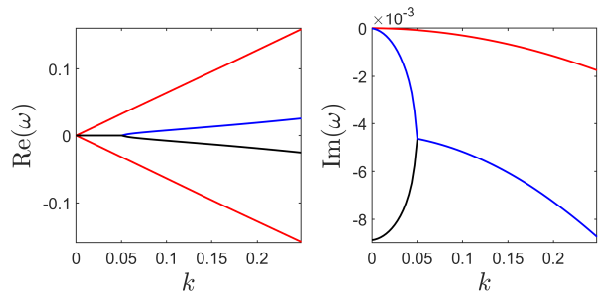


Figure 2. The QNM spectrum for holographic miscible binary superfluids with  $T/T_c = 0.677$ ,  $\nu = -0.1$  and  $v_y = 0$ . Left panel shows real part of QNMs while right panel shows imaginary part. Red lines are sound modes. Blue line and black line correspond to type II Goldstone boson when  $\nu = 0$ . At nonzero  $\nu$ , we expect one branch of this mode to obtain an imaginary gap, which is indeed what we observe.

When the superfluid velocity  $v_y$  is larger than certain critical value  $v_c$ , one of these modes (25) crosses to the upper half plane ( $\text{Im}\omega > 0$ ) and therefore signals a dynamical instability. While

this occurs both for the counterflow and the coflow cases, we will show that the dominant unstable modes are different.

### 1. Dispersion relation for counterflow case

In the counterflow case for which  $\mathbf{v}_1^s = -\mathbf{v}_2^s = (0, v_y)$ , the instability first presents itself in one of the sound modes of (25). More precisely, above the critical velocity  $v_{c1}$ , the sound speed becomes purely imaginary ( $v_s^2 < 0$ ) and one of them obtains a positive imaginary part, see the red lines in the upper panel of Figure 3. There is another critical velocity  $v_{c2}$ , above which the unstable mode becomes gapped at  $k = 0$ , as shown by the black line in the lower panel of Figure 3.

As predicted by the hydrodynamics of binary superfluids in Section II, the onset of thermodynamic instability for is given by (17). Since  $\chi_{+-}=0$  for both counterflow and coflow case, one then has the criterion  $\chi_{++} = 0$  or  $\chi_{--} = 0$ . We find that the former one  $\chi_{++} = \delta^2 f / \delta^2 v_+^s |_{v_-^s} = 0$  explains precisely the dynamical instability we observe in the counterflow case, while  $\chi_{--}$  does not change sign. According to the holographic dictionary, the free energy density  $f$  is computed from the on-shell bulk action with Euclidean signature times temperature. Then we can extract  $\chi_{++}$  by calculating the free energy density for different  $v_+^s$  while keeping  $v_-^s$  fixed. See Appendix C1 for more details. In Figure 4, we plot the sound velocity  $v_s$  and  $\chi_{++}$  for differ-

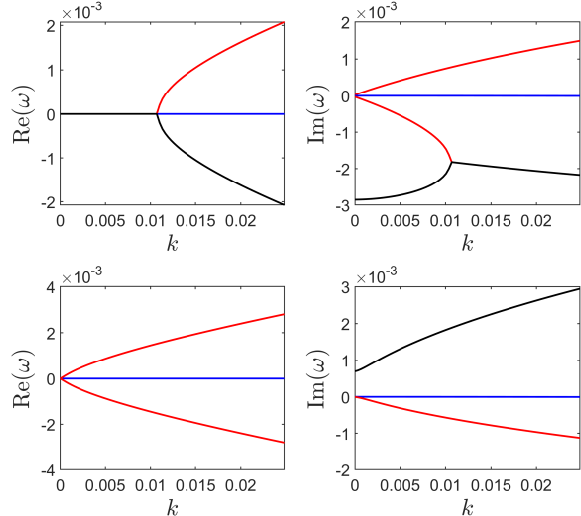


Figure 3. Spectrum of QNMs at low momentum for counterflow case. **Top:** Spectrum of QNMs for superfluid velocity  $v_{y1} = 0.283$ . **Bottom:** Spectrum of QNMs for superfluid velocity  $v_{y2} = 0.314$ . Red lines are sound modes, blue line is diffusive mode and black line is gapped mode. Relevant parameters are  $T/T_c = 0.677$ ,  $\nu = -0.2$ . Note  $v_{c1} < v_{y1} < v_{c2}$  and  $v_{y2} > v_{c2}$ . The unstable mode for  $v_{y1}$  is sound mode, while for  $v_{y2}$ , the unstable mode is the gapped mode. For reference, the two critical velocities at  $T/T_c = 0.677$  and  $\nu = -0.2$  are numerically found to be  $v_{c1} = 0.251$ ,  $v_{c2} = 0.308$ .

ent superfluid velocities  $v_y$ .<sup>8</sup> The two critical velocities  $v_{c1}$  and  $v_{c2}$  are denoted by vertical dashed lines. We see the the first critical velocity corresponds exactly to  $\chi_{++} = 0$ . Note that  $\chi_{n+} \sim v_+^s$ . Therefore  $\chi_{n+} = 0$  for the counter-

<sup>8</sup> In Figure 4, the sound velocity is extracted from QNMs directly by  $v_s = \lim_{k \rightarrow 0} \omega/k$ . One can also extract sound velocity from susceptibilities according to (15). We have verified that results from these two methods agree within numerical error, and the discrepancy is given in Appendix E.

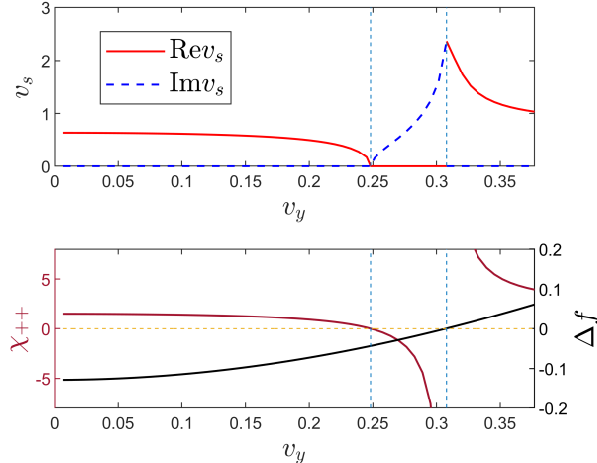


Figure 4. **Top:** Sound velocity of sound mode  $v_s$  for different superfluid velocities  $v_y$  in counterflow case.

**Bottom:** Susceptibility  $\chi_{++}$  and free energy density difference  $\Delta f = f_{\text{binary}} - f_{\text{single}}$ . The vertical dashed lines denote critical velocities  $v_{c1}$  and  $v_{c2}$ . Above  $v_{c1}$ ,  $\chi_{++}$  changes sign, the sound velocity becomes purely imaginary, and one sound mode becomes unstable. Above  $v_{c2}$ ,  $\Delta f$  becomes positive. When  $\Delta f > 0$ , the binary superfluid phase is globally thermodynamically unstable, and the gapped mode becomes unstable with a positive imaginary part at  $k = 0$ . Relevant parameters are  $T/T_c = 0.677$ ,  $\nu = -0.2$ .

flow case, where  $v_+^s = 0$ . Then from (15), the sound velocity is  $v_s = \sqrt{\chi_{++}/\chi_{nn}}$ . One can see the sound velocity should become pure imaginary when  $\chi_{++}$  changes sign, which is exactly what happens to the sound velocity above the first critical velocity (see the dashed blue line of Figure 4).

We point out that the fastest growing mode for above instability develops at a finite wave number. Interestingly, as  $v_y$  is increased,  $\chi_{++}$  becomes positive again, for which hydrodynamics of Section II suggests no instability. Surpris-

ingly, we find that, beyond the second critical velocity  $v_{c2}$ , the system does become unstable at  $k = 0$  while retaining a positive  $\chi_{++}$ . This is a global instability associated with the gapped mode becoming unstable, due to order competition between the two components.<sup>9</sup> Note that there exist two kinds of broken phases: the single superfluid phase and the binary superfluid phase. When  $v_y > v_{c2}$ , the binary superfluid phase becomes less thermodynamically favored and order competing between the two components triggers a global instability. We can verify this by comparing the free energy of the two phases. By calculating the difference of free energy density between the two superfluid phases  $\Delta f = f_{\text{binary}} - f_{\text{single}}$ , we find that  $\Delta f$  becomes positive exactly when  $v_y > v_{c2}$ , see the black line in the bottom panel of Figure 4. Therefore, there will be a first order phase transition from the binary superfluid phase to the single superfluid phase. Moreover, as shown in Figure 4,  $\chi_{++}$  diverges at  $v_{c2}$ . This instability is indeed thermodynamic origin but beyond the scope of our hydrodynamic description.

## 2. Dispersion relation for coflow case

We now turn to the coflow case with  $\mathbf{v}_1^s = \mathbf{v}_2^s = (0, v_y)$ . We first point that the boost symmetry of the GPEs (18) removes the coflow instability for the binary superfluids without relative

<sup>9</sup> Early studies on competing holographic orders can be found, *e.g.* in [27, 28].

velocity. Indeed, at zero temperature where the GPE applies, there is no normal component and any nonzero superfluid velocity can be boosted back using a Galilean transformation to a state where the superfluid is at rest. The holographic setup enjoys relativistic symmetry and is invariant under Lorentz boosts. Nevertheless, at finite temperature, states at nonzero superfluid velocity cannot be boosted back to a state where all components are at rest, since there is a preferred rest frame for the normal component, defined by setting the normal velocity to be  $u^\mu = (1, 0, 0)$ . Indeed, the interface instability for coflow immiscible binary superfluids that is absent in GPE has been recently observed in holographic superfluids [19].

In sharp contrast to the case from GPE (18), we do observe coflow instability from the holographic miscible binary superfluids. More precisely, we find two critical velocities denoted as  $v'_{c1}$  and  $v'_{c2}$ . Comparing with the counterflow case, we find that the binary superfluid phase is always thermodynamically preferred for the coflow case, and thus there is no global instability.

As depicted in the upper panel of Figure 5, the instability first occurs from the diffusive mode of (25) when the superfluid velocity is above  $v'_{c1}$ . Meanwhile, the sound and gapped modes are stable. As the superfluid velocity increases further to above  $v'_{c2}$ , the other instability shows up from one of the sound modes, see red lines in the lower panel of Figure 5. We find

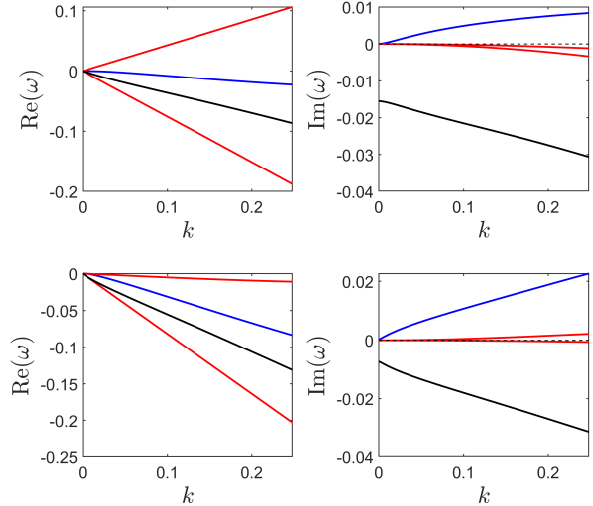


Figure 5. Spectrum of QNMs for coflow case. **Top:** Spectrum of QNMs for superfluid velocity  $v'_{y1} = 1.257$ . **Bottom:** Spectrum of QNMs for superfluid velocity  $v'_{y2} = 2.199$ . Red lines are sound modes, blue line is the diffusive mode and black line is the gapped mode. Relevant parameters are  $T/T_c = 0.677$ ,  $\nu = -0.2$ . Note  $v'_{c1} < v'_{y1} < v'_{c2}$  and  $v'_{y2} > v'_{c2}$ . For  $v'_{y1}$  only the diffusive mode is unstable, while for  $v'_{y2}$ , one of the sound mode also becomes unstable. For reference, the two critical velocities at  $T/T_c = 0.677$  and  $\nu = -0.2$  are numerically found to be  $v'_{c1} = 0.691$ ,  $v'_{c2} = 2.136$ .

that these two critical velocities exactly correspond to  $\chi_{--} = 0$  and  $\chi_{++} = 0$ , respectively. For the coflow case case with  $v_-^s = 0$ , the attenuation is  $\Gamma_0 = -\chi_{--}\delta_1/4$  from (15). Therefore, when  $\chi_{--}$  changes sign, the diffusive mode becomes unstable. Moreover, when  $\chi_{++}$  changes sign, the sound velocity becomes negative, and meanwhile  $\Gamma$  becomes positive. To see this, we expand the sound velocity and attenuation in (15) around  $\chi_{++} = 0$ . Without loss of generality, we assume  $\chi_{n+} > 0$ . Then one of the sound

velocity and attenuation would be

$$v_s = \delta\chi_{++}/2\chi_{n+},$$

$$\Gamma = -\frac{\delta\chi_{++}}{16}(\delta_1 + \delta_2(v_+^s)^2 + \frac{4\beta v_+^s}{\chi_{n+}} + \frac{4\sigma}{\chi_{n+}^2}). \quad (26)$$

Negative  $v_s$  would signal excitation of modes with negative energy, and thus implies energetic instability.

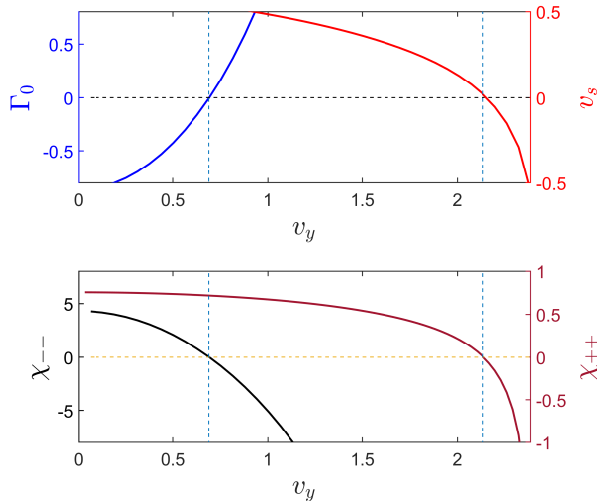


Figure 6. **Top:** Sound velocity  $v_s$  of the unstable sound mode and attenuation  $\Gamma_0$  of the diffusive mode for different superfluid velocities  $v_y$  in coflow case. **Bottom:** susceptibilities  $\chi_{++}$  and  $\chi_{--}$ . The vertical dashed lines denote the critical velocities  $v'_{c1}$  and  $v'_{c2}$ , given by  $\chi_{--} = 0$  and  $\chi_{++} = 0$  respectively. Above  $v'_{c1}$ , the diffusivity changes sign and the diffusive mode becomes unstable. Above  $v'_{c2}$ , the sound mode also becomes unstable, with its velocity and attenuation both changing sign. Relevant parameters are  $T/T_c = 0.677$ ,  $\nu = -0.2$ .

As shown in Figure 6, the above features from hydrodynamics are exactly what happens at the two critical velocities (vertical lines) in the holographic binary superfluids. At  $v'_{c1}$ , both  $\chi_{--}$

and  $\Gamma_0$  vanish and change sign. At the larger critical velocity  $v'_{c2}$ ,  $\chi_{++}$ ,  $v_s$  and  $\Gamma$  change their signs. Note that  $\chi_{--}$  is always negative when  $v_y > v'_{c1}$ . As we mentioned in Appendix D, there are two sets of solutions for the coflow case  $(u_1, v_1) = \pm(u_2, v_2)$ . By checking the eigenfunctions numerically, we find that the sound modes correspond to  $(u_1, v_1) = (u_2, v_2)$ , while the quadratic mode and the gapped mode correspond to  $(u_1, v_1) = -(u_2, v_2)$ . Note  $(u_I, v_I)|_{z=0}$  are just perturbation of condensations on the boundary. This makes the physical meaning of the two kinds of coflow instability clear. For the first instability, perturbations of the two condensates are in the opposite phase, *i.e.* the two components have relative motion. For the second instability, perturbations are in the same phase, *i.e.* the two components move as a whole. In this sense, we can consider the second instability corresponding to the generalization of Landau instability in binary superfluids, which is due to both superfluids moving relative to normal component.

## B. Nonlinear stage for counterflow and coflow instability

From linear analysis we have uncovered that miscible binary superfluids with superflow velocity generically present dynamical instabilities that follow from thermodynamic instabilities. In this section we explore the nonlinear stage of counterflow and coflow instabilities by evolving



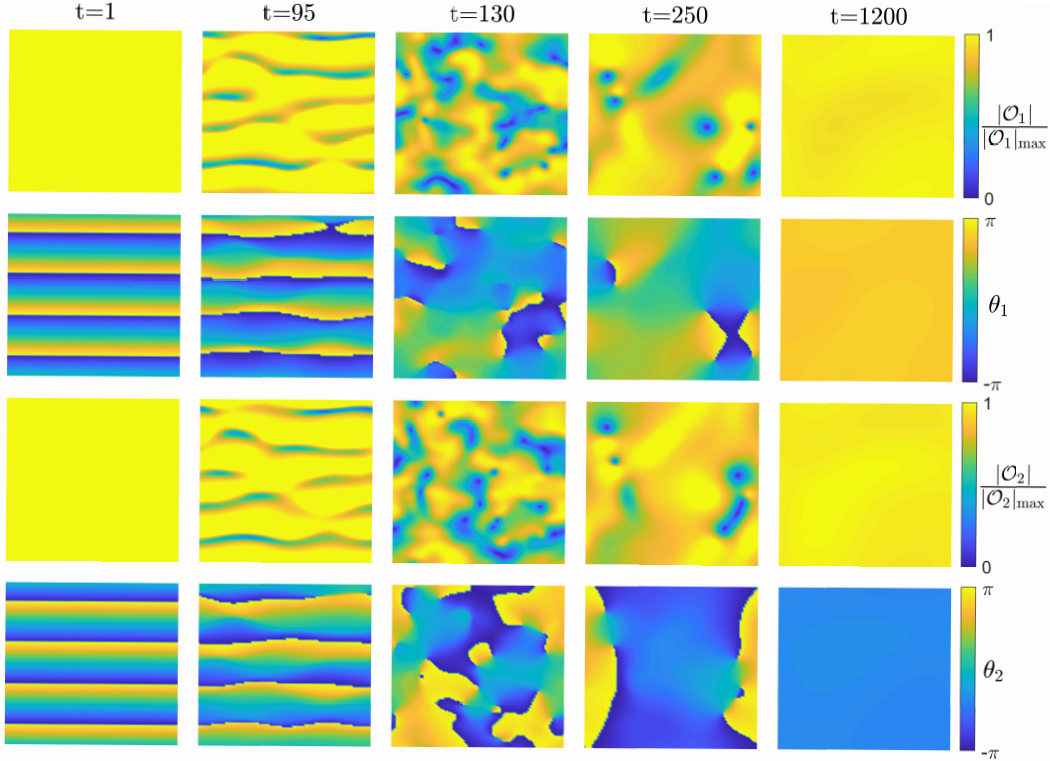


Figure 7. Nonlinear time of counterflow instability at  $T/T_c = 0.677$ ,  $\nu = -0.2$ . Initial superfluid velocity is  $v_y = 0.628$ . Plotted region is  $[0,40] \times [0,40]$ . From top to bottom, plotted values are  $|\mathcal{O}_1|/|\mathcal{O}_1|_{\max}$ ,  $\theta_1$ ,  $|\mathcal{O}_2|/|\mathcal{O}_2|_{\max}$  and  $\theta_2$ . As time goes by, initial small perturbations grows exponentially. Then a dark soliton forms and vortex nucleation occurs. Due to strong dissipation within the system, vortices annihilate with anti-vortices. During this process, the kinetic energy of superfluids is also dissipated and the final state is homogeneous binary superfluids with velocity below critical velocity  $v_{c1}$ . Plotted region is  $[0,40] \times [0,40]$ .

the system forward in time using the full set of nonlinear EoMs. Explicit form of EoMs and time evolution scheme can be found in Appendix B.

In Figure 7 and Figure 8, we show typical examples of such nonlinear time evolution for counterflow and coflow instabilities, respectively. Phenomena for both cases looks similar, except that the coflow instability develops much more slowly and mildly. Since the system is dynamically unstable, small perturbations initially grow exponentially over time and eventually drive the

system into a highly inhomogeneous state. Then nonlinear dynamics takes over and a dark soliton forms. Due to the instability of the dark soliton, vortex nucleation begins to occur. As the vortex number grows, the system is set into full quantum turbulence. In the next stage, due to strong dissipation in holographic superfluids, vortices and anti-vortices annihilate with each other and the total vortex/anti-vortex number gradually decreases. During this process, the kinetic energy of superfluids is also dissipated and



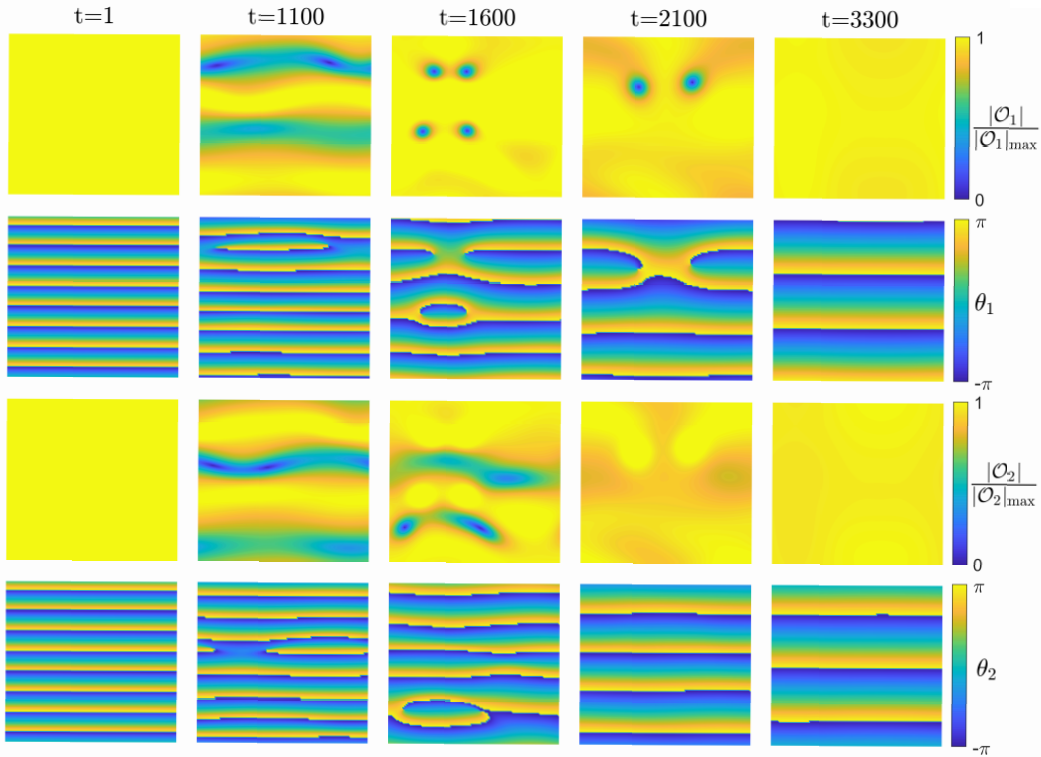


Figure 8. Nonlinear evolution of coflow instability at  $T/T_c = 0.677$ ,  $\nu = -0.2$ . Initial superfluid velocity is  $v_y = 1.257$ . The same values and regions are plotted as those for counterflow case. Phenomenon is similar to that of counterflow case, except coflow instability develops much more slowly and mildly. The final state is homogeneous binary superfluids with velocity below critical velocity  $v'_{c1}$ .

the overall superfluid velocity is lowered. After a long time, when vortices are all annihilated, the final state of system is again a homogeneous binary superfluid, but with a superfluid velocity below the critical velocity, which is  $v_{c1}$  for the counterflow case and  $v'_{c1}$  for the coflow case. Such slowing down mechanism might be universal for dissipative superfluids. In single-component superfluids, the superfluid velocity is also lowered to below the Landau critical velocity by vortex nucleation and annihilation [29].

## V. UNIVERSAL SCALING LAW OF CRITICAL VELOCITY

While we have shown some key differences between the GPEs and the holographic description for binary superfluids, both share a similar scaling law of critical velocity.

When the two components are identical, as is the case in the present work, the critical velocity of counterflow instability from the coupled GPEs (18) was found to be [8–11]

$$v_c \sim \sqrt{1 - \Delta^2}, \quad \Delta = g_{12}/\sqrt{g_1 g_2}. \quad (27)$$

In the holographic theory, we have uncovered

four critical velocities:  $v_{c1}$ ,  $v_{c2}$  for counterflow case and  $v'_{c1}$ ,  $v'_{c2}$  for coflow case. Interestingly, we find three of the four critical velocities scale as  $\nu^{1/2}$ , see Figure 9. And this scaling behavior persists for all temperatures. The only velocity which does not follow this scaling behavior is the critical velocity  $v'_{c2}$ .  $v'_{c2}$  is nonzero even when  $\nu$  vanishes and barely changes as  $\nu$  decreases. This can be understood as that  $v'_{c2}$  corresponds to Landau critical velocity which is due to the whole superfluid moving relative to the normal component and thus persists even the two components do not interact.

Such similar scaling behavior between the two models prompts us to identify  $\nu$  with  $1 - \Delta^2$ . In the recent work about interface instability of immiscible binary superfluids by some of us [18], similar scaling behavior for interface width between the two models was found for small  $\nu$  by identifying  $\nu$  with  $1 - \Delta$ . In fact, the two identifications are equivalent for small  $\nu$ . If we take  $\nu = 1 - \Delta^2$ , for small  $\nu$  we would have

$$1 - \Delta = 1 - \sqrt{1 - \nu} = \frac{1}{2}\nu + \mathcal{O}(\nu^2). \quad (28)$$

The coefficient  $1/2$  has no effect on scaling laws. It is nontrivial to find the same identification and scaling law between weakly interacting and strongly interacting binary superfluids independently in dynamical instability analysis of miscible binary superfluids and stationary state of immiscible binary superfluids. This result suggests that the scaling law for critical velocity might be universal, no matter whether the superfluid

is weakly interacting or strongly interacting.

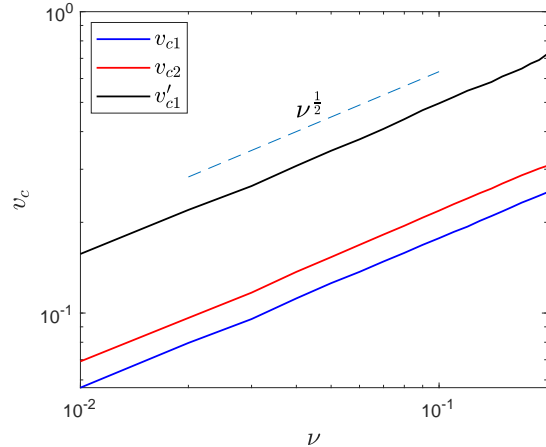


Figure 9. Two critical velocities  $v_{c1}$ ,  $v_{c2}$  for counterflow case and the first critical velocity  $v'_{c1}$  for coflow case versus coupling strength  $\nu$  at  $T/T_c = 0.677$ . All critical velocities scale as  $\nu^{1/2}$ . This result also holds at other temperatures.

## VI. CONCLUSION AND DISCUSSION

We have studied the counterflow and coflow instabilities in miscible binary superfluids. The former one is general in two-component fluid systems, while the latter instability is only presented in non-Galilean invariant systems, such as dissipative systems. We first developed a hydrodynamic framework for binary superfluids in Section II. Based in the local thermodynamic stability and positivity of entropy production, we have shown that binary superfluids become linearly dynamically unstable whenever the matrix of static susceptibility  $\chi_{AB}$  is no longer positive definite.

We have demonstrated that the dynamical

counterflow instability found from GPEs is essentially captured by our criterion and thus this instability is of thermodynamic origin. In the framework of GPE, there is no coflow instability in an isolated uniform system because of Galilean invariance. In contrast to GPE, the holographic superfluids describes strongly coupled superfluids at finite temperature and dissipation. We found rich dynamics from the holographic miscible binary superfluids.

From linear analysis, we have found that for both counterflow and coflow cases, dynamical instability only occurs above some critical superfluid velocity, see *e.g.* Figures 3 and 5. It first occurs in sound mode for the counterflow case, while in dissipative mode for coflow case. As the superfluid velocity further increases, another critical velocity shows for each case. For the counterflow case, the presence of the additional critical velocity is due to order competing mechanism between the two components. Above the second critical velocity, free energy of the counterflow binary superfluid phase is higher than that of single component phase, therefore the binary superfluid phase becomes less thermodynamically favored. In accordance, the unstable mode above the second critical velocity becomes the gapped mode, which is unstable even at zero wave number, signaling a global instability. For coflow case, the second critical velocity corresponds to Landau critical velocity in single component superfluids. Above this critical velocity, one of the sound modes also becomes unstable.

Nevertheless, the unstable dissipative mode always dominates the instability.

By formulating hydrodynamics of binary superfluids, we have found that except  $v_{c2}$ , which is due to order competing, other three instabilities originate in the divergences of susceptibility matrix  $\chi_{AB}$ . In this sense, all these instabilities are thermodynamic origin.

Then we have explored the nonlinear stage of these dynamical instabilities by evolving the systems forward in time. We found the phenomena for two kinds of instabilities are similar, see Figures 7 and 8. In linear stage, small perturbations grow exponentially and drive the system into inhomogeneous state and then nonlinearity takes over. Firstly, dark soliton forms. Due to instability of dark soliton, vortex nucleation occurs. Then overall velocity of the system is reduced due to vortex annihilation and dissipation. The final state of the evolution is a homogeneous binary superfluid with velocity below critical velocity. Such mechanism seems to be general in dissipative superfluids.

We have limited ourselves to the superfluids with identical components under the simplifying assumption of colinearity. Nevertheless, there should be no conceptual obstacle generalising to general cases. Moreover, it is desirable to understand the range of application of the hydrodynamic framework. In particular, one could expand the hydrodynamic expansion to higher orders to compare with the non-linear stage of the system. In following work, we shall also

explore properties of vortex in strongly interacting miscible binary superfluids and compare them with those of weakly interacting binary superfluids [30–32]. While we have uncovered the thermodynamic origin of counterflow and coflow instabilities in miscible binary superfluids, it would be interesting to generalize the discussion to the immiscible binary superfluids, for which one has to deal with a phase-separated configuration. The tension from the interface could play an important role for the instability of the system [33].

### ACKNOWLEDGMENTS

This work was partly supported by the National Natural Science Foundation of China Grants No.12075298, No.12122513, No.11991052 and No.12047503. We thank Jilin University for hospitality during the School of Frontiers in Hydrodynamics, Effective Field Theory and Holographic Duality. We acknowledge the use of the High Performance Cluster at Institute of Theoretical Physics, Chinese Academy of Sciences.

### Appendix A: Holographic setup

The holographic 2 + 1-dimensional binary superfluid model reads [18]

$$\begin{aligned} \mathcal{L} = & -(\mathcal{D}_\mu \Psi_1)^* \mathcal{D}^\mu \Psi_1 - m_1^2 |\Psi_1|^2 - (\mathcal{D}_\mu \Psi_2)^* \mathcal{D}^\mu \Psi_2 \\ & - m_2^2 |\Psi_2|^2 - \frac{\nu}{2} |\Psi_1|^2 |\Psi_2|^2 - \frac{1}{4} F^{\mu\nu} F_{\mu\nu}, \end{aligned} \quad (\text{A1})$$

where  $\mathcal{D}_\mu \Psi_I = (\nabla_\mu - ie_I A_\mu) \Psi_I$ ,  $A_\mu$  is the  $U(1)$  gauge field,  $F_{\mu\nu}$  is the field strength and  $\Psi_{I\text{S}}$  are two complex scalar fields coupled with each other. As is mentioned in previous work by some of us [18], this model corresponds to immiscible binary superfluid for  $\nu > 0$  and miscible binary superfluid for  $\nu < 0$ . In terms of the background, we utilize a 3 + 1-dimensional planar AdS black hole described in Eddington-Finkelstein coordinates:

$$ds^2 = \frac{L^2}{z^2} (-(1 - (z/z_h)^3) dt^2 - 2 dt dz + dx^2 + dy^2). \quad (\text{A2})$$

The dual field theory coordinates are  $(t, x, y)$  while  $z$  is the holographic radial coordinate, with the boundary located at  $z = 0$  and the black hole horizon at  $z = z_h$ . This represents a heat bath at the boundary with temperature  $T = 3/(4\pi z_h)$ . For simplicity, we set  $L = z_h = 1$ ,  $m_1^2 = m_2^2 = -2$ ,  $e_1 = e_2 = 1$ , and adopt the radial gauge  $A_z = 0$ .

Consequently, the asymptotic expansions for  $A_\mu$  and  $\Psi_I$  near the AdS boundary are:

$$\begin{aligned} A_\mu &= a_\mu + b_\mu z + \mathcal{O}(z^2), \\ \Psi_I &= (\Psi_I)_0 z + (\Psi_I)_1 z^2 + \mathcal{O}(z^3). \end{aligned} \quad (\text{A3})$$

In the context of gauge-gravity duality, the coefficients  $a_t$ ,  $a_i$  ( $i = x, y$ ), and  $(\Psi_I)_0$  can be recognized as the chemical potential  $\mu$ , vector potential, and scalar operator source at the boundary, respectively.  $(\Psi_I)_1$  corresponds to the expectation value of the order parameter  $\langle \hat{\mathcal{O}}_I \rangle$ . In our study, we work within the grand-canonical ensemble, *i.e.* by fixing  $\mu$ , without considering al-

ternative quantization. It is important to note that  $T$  and  $\mu$  are not independent quantities due to the scaling symmetry of the system. After setting  $z_h = 1$ ,  $\mu$  becomes the sole free parameter. A second-order phase transition occurs in this model when  $\mu \geq \mu_c \simeq 4.064$ , which also determines the ratio  $T/T_c = \mu_c/\mu$ .

To investigate holographic superfluids with spontaneously broken symmetry, we turn off electromagnetic fields and scalar sources at the boundary, meaning  $a_x = a_y = (\Psi_I)_0 = 0$ . Consequently, the charge conservation equation at

the boundary is given by  $-\partial_t b_t = b_i$ , where  $-b_t = n$  represents the charge density and  $b_i = j_i$  is the charge current. The superfluid velocity is determined by  $\mathbf{v}^s = \nabla\theta|_{z=0}$ , where  $\theta$  is the phase (the Goldstone field) of the order parameter  $\langle \hat{\mathcal{O}} \rangle$ .

## Appendix B: Equations of motion and time evolution scheme

The explicit form of equations of motion (EoMs) for  $\Psi_I$  and  $A_\mu$  are

$$2\partial_t\partial_z\Phi_I - [2iA_t\partial_z\Phi_I + i\partial_zA_t\Phi_I + \partial_z(f\partial_z\Phi_I) - z\Phi_I + \partial_x^2\Phi_I + \partial_y^2\Phi_I - i(\partial_xA_x + \partial_yA_y)\Phi_I - (A_x^2 + A_y^2)\Phi_I - 2i(A_x\partial_x\Phi_I + A_y\partial_y\Phi_I) - \frac{\nu}{2}|\Phi_j|^2\Phi_I] = 0, \quad (i, j = 1, 2, \quad i \neq j) \quad (\text{B1})$$

$$\partial_t\partial_zA_t - [\partial_x^2A_t + \partial_y^2A_t + f\partial_z(\partial_xA_x + \partial_yA_y) - \partial_t(\partial_xA_x + \partial_yA_y) - 2A_t\sum_I|\Phi_I|^2 - 2f\text{Im}(\sum_I\Phi_I^*\partial_z\Phi_I) + 2\text{Im}(\sum_I\Phi_I^*\partial_t\Phi_I)] = 0, \quad (\text{B2})$$

$$2\partial_t\partial_zA_x - [\partial_z(\partial_xA_t + f\partial_zA_x) + \partial_y(\partial_yA_x - \partial_xA_y) - 2A_x\sum_I|\Phi_I|^2 + 2\text{Im}(\sum_I\Phi_I^*\partial_x\Phi_I)] = 0, \quad (\text{B3})$$

$$2\partial_t\partial_zA_y - [\partial_z(\partial_yA_t + f\partial_zA_y) + \partial_x(\partial_xA_y - \partial_yA_x) - 2A_y\sum_I|\Phi_I|^2 + 2\text{Im}(\sum_I\Phi_I^*\partial_y\Phi_I)] = 0, \quad (\text{B4})$$

$$\partial_z(\partial_xA_x + \partial_yA_y - \partial_zA_t) - 2\text{Im}(\sum_I\Phi_I^*\partial_z\Phi_I) = 0, \quad (\text{B5})$$

where  $\Phi_I = \Psi_I/z$  and  $\text{Im}$  represents imaginary part. Notice the last equation is a constraint with no time derivative. These equations are not independent. They obey the following constraint

equation

$$-\partial_t\text{Eq.}(\text{B5}) - \partial_z\text{Eq.}(\text{B2}) + \partial_x\text{Eq.}(\text{B3}) + \partial_y\text{Eq.}(\text{B4}) = 2\text{Im}(\sum_I\text{Eq.}(\text{B1}) \times \Phi_{0I}^*). \quad (\text{B6})$$

The initial condition is set to be stationary geometry (A2):  
mixture perturbed by some random noise:

$$\Phi_I = \Phi_{0I} e^{i(v_I)_y y} (1 + \alpha n(x, y)), \quad (\text{B7})$$

where  $\alpha$  is a small number set to be  $10^{-3}$ , and  $n(x, y)$  is the random noise superimposed on the stationary background.

For time evolution, we use fourth order Runge-Kutta method and the following scheme: First, we use (B1), (B3) and (B4) to evolve  $\Phi$ ,  $A_x$  and  $A_y$  with boundary conditions  $\Phi(z=0) = A_x(z=0) = A_y(z=0) = 0$ . Then we use (B2) to evolve  $\partial_z A_t$  on the boundary. Note that  $-\partial_z A_t(z=0)$  is just the charge density or number density  $\rho$  of the dual field theory. Finally, we use (B5) to solve  $A_t$  by evolved  $\Phi$ ,  $A_x$ ,  $A_y$  and boundary conditions  $\partial_z A_t(z=0) = -\rho$  and  $A_t(z=0) = \mu$ . Such scheme keeps  $\mu$ , the chemical potential, unchanged, so we are in fact working in grand canonical ensemble. In  $z$  direction, we use Chebyshev pseudo spectral method. In  $x$  and  $y$  direction we use Fourier pseudo spectral method and periodic boundary condition.

### Appendix C: Stationary miscible binary superfluids

Stationary configuration for miscible binary superfluids is homogeneous in spatial directions. We choose the following ansatz around the bulk

$$\begin{aligned} \Psi_I &= z \phi_I(z) e^{i\Theta_I(z,x,y)}, \\ A_t &= A_t(z), \\ V_{Ix}(z) &\equiv \partial_x \Theta_I - A_x, \\ V_{Iy}(z) &\equiv \partial_y \Theta_I - A_y, \\ (I &= 1, 2), \end{aligned} \quad (\text{C1})$$

together with the gauge  $\partial_z \Theta_I = -A_t/f$ . The consistence of above ansatz requires  $\partial_z(A_y + V_{Iy}) = 0$  and  $\partial_z(A_x + V_{Ix}) = 0$ . Note that the phase  $\Theta_I$  of the condensation  $\mathcal{O}_i$  corresponds to  $\Theta_I|_{z=0}$ . According to the holographic dictionary, we have  $\mathbf{V}_I|_{z=0} = \mathbf{v}_I^s$ , where  $\mathbf{v}_I^s$  is the superfluid velocity of  $I$ -th component. If  $\mathbf{v}_I$  does not depend on spatial and radial coordinates, as is the case in this work, we would have  $\mathbf{V}_I = \mathbf{v}_I - \mathbf{A}$  and  $\Theta_I(z, x, y) = \Theta(z) + (v_I^s)_x x + (v_I^s)_y y$ .

The resulting bulk EoMs are given as

$$\begin{aligned} \partial_z(f \partial_z \phi_I) - (V_{Ix}^2 + V_{Iy}^2) \phi_I + \frac{A_t^2}{f} \phi_I \\ - z \phi_I - \frac{\nu}{2} \phi_J^2 \phi_I &= 0, \quad (I \neq J), \\ f \partial_z^2 A_t - 2A_t \sum_I \phi_I^2 &= 0, \\ \partial_z(f \partial_z V_{Ix}) - 2 \sum_I V_{ix} \phi_I^2 &= 0, \\ \partial_z(f \partial_z V_{Iy}) - 2 \sum_I V_{Iy} \phi_I^2 &= 0, \end{aligned} \quad (\text{C2})$$

which involves 7 coupled ordinary differential equation for  $(\phi_I, V_{Ix}, V_{Iy}, A_t)$  that depend on the variables  $z$  only. The boundary conditions at the AdS boundary  $z=0$  read

$$\begin{aligned} \phi_I(z=0) &= 0, \quad A_t(z=0) = \mu, \\ V_{Ix}(z=0) &= (v_I^s)_x, \quad V_{Iy}(z=0) = (v_I^s)_y. \end{aligned} \quad (\text{C3})$$

We consider the regular condition at the event horizon  $z = 1$ . Then, we solve the above equations numerically by adopting the Newton-Raphson method together with the Chebyshev pseudo-spectral method. In this work, we focus on the cases where  $\mathbf{v}_1^s/\mathbf{v}_2^s$ . Without loss of generality, we assume that they are along the  $y$  direction.

Apparently, there exists two kinds of solution. One is single component superfluid solution  $\phi_I \neq 0$ ,  $\phi_J = 0$ , and the other is binary superfluid solution, which is the focus of this work. For fixed temperature, binary superfluid solution only exists for  $\nu > \nu_c$  [34]. Below this critical value, superfluid would collapse due to strong attraction between the two components. For counterflow case  $v_+ = 0$  and coflow case  $v_- = 0$ , there is a additional symmetry  $\phi_1 = \phi_2 = \phi$  between the two components. Utilizing the symmetry, the EoMs (C2) can be slightly further simplified. For counterflow binary superfluids  $(v_1)_y = -(v_2)_y = v_y$ , the difference of the two equations for  $\phi_I$  gives  $v_y A_y \phi = 0$ , which means  $A_y = 0$  for nonzero  $\phi$ . Then, the equation of motion for  $V_{Iy}$  are eliminated, and the full EoMs become

$$\begin{aligned} \partial_z(f\partial_z\phi) - v_y^2\phi + \frac{A_t^2}{f}\phi - z\phi - \frac{\nu}{2}\phi^3 &= 0, \\ f\partial_z^2 A_t - 4A_t\phi^2 &= 0. \end{aligned} \quad (\text{C4})$$

Note that these are not identical to EoMs of the single component holographic superfluid, since equation for  $A_y$  is absent. For coflow binary superfluids  $(v_1)_y = (v_2)_y = v_y$ , the two compo-

nents are completely identical. We would also have  $V_{1y} = V_{2y} = V_y$ . In this case, the EoMs are

$$\begin{aligned} \partial_z(f\partial_z\phi) - V_y^2\phi + \frac{A_t^2}{f}\phi - z\phi - \frac{\nu}{2}\phi^3 &= 0, \\ f\partial_z^2 A_t - 4A_t\phi^2 &= 0, \\ \partial_z(f\partial_z V_y) - 4V_y\phi_I^2 &= 0, \end{aligned} \quad (\text{C5})$$

which are identical to the EoMs of the single component superfluid with extra self interaction  $\nu' = \nu/2$  and the superfluid velocity  $v_y$  if we rescale the scalar field  $\phi \rightarrow \phi/\sqrt{2}$ . Nevertheless, in the main text we have seen that the presence of the second component introduces additional instability into the system beside the Landau instability of single component superfluids.

### 1. Free energy density and susceptibilities

Given the stationary solutions, we can proceed to calculate the free energy density and susceptibilities. According to the holographic dictionary, the free energy is simply identified with on-shell bulk action with Euclidean signature times temperature. In the probe limit with sources of condensates set to 0, we can neglect the gravity part of the action, the Euclidean action is finite and no counter term is needed. Therefore the free energy density can easily be calculated as

$$f = - \int dz \sqrt{-g} \mathcal{L}_{\text{on-shell}}. \quad (\text{C6})$$

where  $\mathcal{L}$  is given by (A1). This is essentially the free energy density difference with respect to pure AdS planar black hole without matter



fields. To get  $\chi_{AB}$ , which is given by

$$\chi_{AB} = \frac{\delta^2 f}{\delta s_A \delta s_B}, \quad (\text{C7})$$

we need to calculate the free energy density for different  $s_A$  and  $s_B$ . In this work,  $f$  depends on three parameters  $s = (\mu, v_+^s, v_-^s)$ . Once we get  $f(\mu, v_+^s, v_-^s)$ , we can use finite difference method to extract the value of  $\chi_{AB}$  numerically. For instance, if we want to calculate  $\chi_{++}$ , we need to calculate free energy density for different  $v_+^s$  while keeping  $(\mu, v_-^s)$  fixed to  $(\mu_0, v_{-0}^s)$ , and then calculate  $\partial_{v_+^s}^2 f(\mu_0, v_+^s, v_{-0}^s)$  numerically.

#### Appendix D: Linearized equations of motion

In this section we consider dynamical counterflow and coflow instabilities in miscible holographic binary superfluids using linear response theory. We turn on small perturbations on the

stationary background

$$\begin{aligned} \Phi_I &= (\Phi_{I0} + \delta\Phi_i) e^{i(v_I)_y y}, \\ A_t &= A_{t0} + \delta A_t, \\ A_y &= A_{y0} + \delta A_y, \end{aligned} \quad (\text{D1})$$

and linearize the EoMs (B1)-(B5). Here  $\Phi_{0I} = \phi_I e^{i\Theta_I}$ ,  $A_{t0}$ ,  $A_{x0}$  and  $A_{y0}$  are stationary solutions solved in last section. Taking into account the translation invariance of the background along the time and spatial directions, we express the bulk perturbation fields as

$$\begin{aligned} \delta\Phi_I &= u_i(z) e^{-i(\omega t - \mathbf{k} \cdot \mathbf{x})}, & \delta\Phi_I^* &= v_i(z) e^{-i(\omega t - \mathbf{k} \cdot \mathbf{x})}, \\ \delta A_t &= a_t(z) e^{-i(\omega t - \mathbf{k} \cdot \mathbf{x})}, & \delta A_y &= a_y(z) e^{-i(\omega t - \mathbf{k} \cdot \mathbf{x})}. \end{aligned} \quad (\text{D2})$$

For simplicity, in this work we only consider wave vectors parallel to the superfluid velocity, *i.e.*  $\mathbf{k} \cdot \mathbf{x} = ky$ .

The full set of linear perturbation equations are given explicitly as

$$\begin{aligned} &2iA_{t0}\partial_z u_I + 2ia_t\partial_z\Phi_{0I} + i\partial_z A_{t0}u_I + i\partial_z a_t\Phi_{0I} + \partial_z(f\partial_z u_I) - zu_I \\ &- (k + (v_I)_y)^2 u_I + k\Phi_{0I}a_y - A_{y0}^2 u_I - 2A_{y0}\Phi_{0I}a_y + 2(k + (v_I)_y)A_{y0}u_I \\ &+ 2a_y(v_I)_y\Phi_{0I} - \frac{\nu}{2}|\Phi_{0j}|^2 u_I - \frac{\nu}{2}\Phi_{0j}^*\Phi_{0I}u_j - \frac{\nu}{2}\Phi_{0j}\Phi_{0I}v_j \\ &= -2i\omega\partial_z u_I, \quad (I, J = 1, 2 \quad I \neq J), \end{aligned} \quad (\text{D3})$$

$$\begin{aligned} &-2iA_{t0}\partial_z v_I - 2ia_t\partial_z\Phi_{0I}^* - i\partial_z A_{t0}v_I - i\partial_z a_t\Phi_{0I}^* + \partial_z(f\partial_z v_I) - zv_I \\ &- (k - (v_I)_y)^2 v_I - k\Phi_{0I}^*a_y - A_{y0}^2 v_I - 2A_{y0}\Phi_{0I}^*a_y - 2(k - (v_I)_y)A_{y0}v_I \\ &+ 2a_y(v_I)_y\Phi_{0I}^* - \frac{\nu}{2}|\Phi_{0j}|^2 v_I - \frac{\nu}{2}\Phi_{0j}\Phi_{0I}^*v_j - \frac{\nu}{2}\Phi_{0j}^*\Phi_{0I}u_j \\ &= -2i\omega\partial_z v_I, \quad (I, J = 1, 2 \quad I \neq J), \end{aligned} \quad (\text{D4})$$

$$\begin{aligned}
& -k^2 a_t + ikf \partial_z a_y - 2a_t \sum_I |\Phi_{0I}|^2 - 2A_{t0} \sum_I (\Phi_{0I}^* u_I + \Phi_{0I} v_I) + if \sum_I (\Phi_{0I}^* \partial_z u_I \\
& - \Phi_{0I} \partial_z v_I + v_I \partial_z \Phi_{0I} - u_I \partial_z \Phi_{0I}^*) = -i\omega (\partial_z a_t + ik a_y) + \omega \sum_I (\Phi_{0I}^* u_I - \Phi_{0I} v_I), \tag{D5}
\end{aligned}$$

$$\begin{aligned}
& ik \partial_z a_t + \partial_z (f \partial_z a_y) - 2a_y \sum_I |\Phi_{0I}|^2 - 2A_{y0} \sum_I (\Phi_{0I}^* u_I + \Phi_{0I} v_I) \\
& + \sum_I ((k + (v_I)_y) \Phi_{0I}^* u_I - (k - (v_I)_y) \Phi_{0I} v_I + (v_I)_y v_I \Phi_{0I} + (v_I)_y u_I \Phi_{0I}^*) \tag{D6} \\
& = -2i\omega \partial_z a_y.
\end{aligned}$$

For more stable numerical performance, we use the following equation for  $a_t$ :

$$\begin{aligned}
\partial_z (ika_y - \partial_z a_t) + i \sum_I (\Phi_I^* \partial_z u_I + v_I \partial_z \Phi_I \\
- u_I \partial_z \Phi_I^* - \Phi_I \partial_z v_I) = 0, \tag{D7}
\end{aligned}$$

which comes from the constraint equation (B5). Moreover, we require (D5) to be satisfied at the AdS boundary  $z = 0$ , yielding

$$(k \partial_z a_y + \omega \partial_z a_t = 0)|_{z=0}. \tag{D8}$$

Then, by considering (B6), (D5) is also satisfied in the whole bulk. Regarding other perturbed fields, we impose the source free boundary condition at the AdS boundary. Finally, the system results in a generalized eigenvalue problem:

$$M_k u_k = i\omega_k B u_k, \quad u_k = \{u_1, v_1, u_2, v_2, a_t, a_y\}_k^T. \tag{D9}$$

The corresponding QNMs are extracted by solving the above generalized eigenvalue problem. Then we can numerically obtain  $\omega$  for each  $k$  and velocity  $v_y$ . Due to dissipation into the normal component, the quasi-normal frequencies

generically take a complex value. Since  $\delta\Phi_I \sim e^{-i\omega t}$ , the stationary configuration will become dynamically unstable whenever  $\text{Im}(\omega) > 0$ . The larger the positive imaginary part is, the more unstable the system becomes.

There are some general features of this generalized eigenvalue problem. Two types of symmetries lie in the EoMs. The first one links EoMs for  $k$  and  $-k$ . If  $u_k$  and  $\omega_k$  is a solution for (D9), we would also have

$$M_{-k} u'_k = -i\omega_k^* u'_k, \quad u'_k = \{v_1, u_1, v_2, u_2, a_t, a_y\}_k^T, \tag{D10}$$

which means  $u_{-k} = u'_k$ ,  $\omega_{-k} = -\omega_k^*$ . The second symmetry originates from the symmetry between the two components. For  $(v_1)_y = \pm(v_2)_y$ , we have

$$\begin{aligned}
M_{\pm k} (\Phi_{01} \leftrightarrow \Phi_{02}, A_y \rightarrow \pm A_y) u_k^\pm = i\omega_k u_k^\pm, \\
u_k^\pm = \{u_2, v_2, u_1, v_1, a_t, \pm a_y\}_k^T. \tag{D11}
\end{aligned}$$

Taking into account  $\Phi_{01} = \Phi_{02}$  and  $A_y = 0$  for  $(v_1)_y = -(v_2)_y$ , we get  $M_{\pm k} (\Phi_{01} \leftrightarrow \Phi_{02}, A_y \rightarrow \pm A_y) = M_{\pm k}$ . Then, combining (D10) and (D11), for counterflow case one

gets

$$\begin{aligned} M_k \bar{u}_k^- &= -i\omega_k^* \bar{u}_k^-, \\ \bar{u}_k^- &= \{v_2, u_2, v_1, u_1, a_t, -a_y\}_k^\dagger. \end{aligned} \quad (\text{D12})$$

Therefore for counterflow case,  $\omega_k$  and  $-\omega_k^*$  comes as pairs for given  $k$ . If  $\omega_k = -\omega_k^*$ , *i.e.*  $\omega_k$  is pure imaginary, we would also have  $(u_1, v_1) = (v_2, u_2)^* e^{i\alpha}$ , where  $\alpha$  is a global phase. For coflow case, we have  $u_k = u_k^\dagger$ , which gives  $(u_1, v_1) = (u_2, v_2) e^{i\alpha} = (u_1, v_1) e^{2i\alpha} \Rightarrow e^{i\alpha} = \pm 1$ . Therefore, there are two sets of solutions  $(u_1, v_1) = \pm(u_2, v_2)$  for coflow case. In the main text, we see that one of the solutions shows Landau instability and the other shows coflow instability.

### Appendix E: Sound velocity from QNMs and susceptibilities

In Figure 4 and Figure 6, we plot the sound velocity extracted from QNMs directly by  $v_s = \lim_{k \rightarrow 0} \omega/k$ . According to (15), one can also extract the sound velocity from the susceptibilities:

$$(v_s)_\pm = \frac{-\chi_{n+} \pm \sqrt{\chi_{n+}^2 + \chi_{++}\chi_{nn}}}{\chi_{nn}}, \quad (\text{E1})$$

with  $\chi_{AB} = \delta^2 f / \delta s_A \delta s_B$ . Sound velocity extracted from these two methods should coincide with each other. As a self consistency check, below in Figure 10, we plot the discrepancy between sound velocities from the two methods  $\Delta v_s / (v_s)_{\text{QNM}} = ((v_s)_{\text{QNM}} - (v_s)_{\text{susceptibility}}) / (v_s)_{\text{QNM}}$  for the larger sound velocity of counterflow and coflow cases separately. We see the results agree well within numerical error.

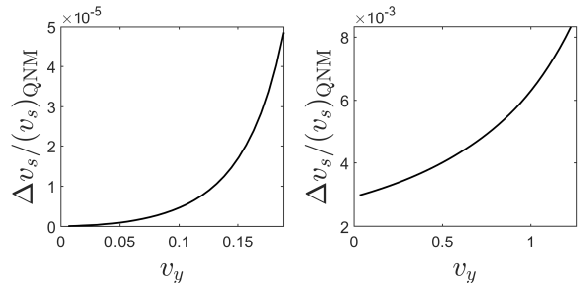


Figure 10. Discrepancy between sound velocities extracted from QNMs and susceptibilities,  $\Delta v_s / (v_s)_{\text{QNM}} = ((v_s)_{\text{QNM}} - (v_s)_{\text{susceptibility}}) / (v_s)_{\text{QNM}}$ , for different superfluid velocities. **Left:** discrepancy of the larger sound velocity of counterflow case. **Right:** discrepancy of the larger sound velocity of coflow case. Relevant parameters are  $T/T_c = 0.677$  and  $\nu = -0.2$ .

[1] Helmholtz, *The London, Edinburgh, and Dublin Philosophical Magazine and Journal of Science* **36**, 337 (1868).  
 [2] W. Thomson, *The London, Edinburgh, and Dublin Philosophical Magazine and Journal of Science* **42**, 362 (1871).

[3] H. Takeuchi, N. Suzuki, K. Kasamatsu, H. Saito, and M. Tsubota, *Physical Review B* **81**, 094517 (2010).  
 [4] G. E. Volovik, *Journal of Experimental and Theoretical Physics Letters* **75**, 418 (2002).  
 [5] R. Blaauwgeers, V. B. Eltsov, G. Eska, A. P. Finne, R. P. Haley, M. Krusius, J. J. Ruohio,

- L. Skrbek, and G. E. Volovik, *Phys. Rev. Lett.* **89**, 155301 (2002).
- [6] A. P. Finne, V. B. Eltsov, R. Hänninen, N. B. Kopnin, J. Kopu, M. Krusius, M. Tsubota, and G. E. Volovik, *Reports on Progress in Physics* **69**, 3157 (2006).
- [7] V. B. Eltsov, A. Gordeev, and M. Krusius, *Phys. Rev. B* **99**, 054104 (2019).
- [8] M. Abad, A. Recati, S. Stringari, and F. Chevy, *The European Physical Journal D* **69**, 126 (2015).
- [9] C. K. Law, C. M. Chan, P. T. Leung, and M. C. Chu, *Physical Review A* **63**, 063612 (2001).
- [10] S. Ishino, M. Tsubota, and H. Takeuchi, *Phys. Rev. A* **83**, 063602 (2011).
- [11] H. Takeuchi, S. Ishino, and M. Tsubota, *Physical Review Letters* **105**, 205301 (2010).
- [12] A. Schmitt, *Phys. Rev. D* **89**, 065024 (2014).
- [13] M. Delehaye, S. Laurent, I. Ferrier-Barbut, S. Jin, F. Chevy, and C. Salomon, *Phys. Rev. Lett.* **115**, 265303 (2015).
- [14] N. Andersson, G. L. Comer, and R. Prix, *Monthly Notices of the Royal Astronomical Society* **354**, 101 (2004).
- [15] A. Haber, A. Schmitt, and S. Stetina, *Physical Review D* **93**, 025011 (2016).
- [16] S. A. Hartnoll, A. Lucas, and S. Sachdev, [arXiv:1612.07324 \[hep-th\]](https://arxiv.org/abs/1612.07324).
- [17] J. Zaanen, Y. Liu, Y.-W. Sun, and K. Schalm, *Holographic Duality in Condensed Matter Physics* (Cambridge University Press, Cambridge, 2015).
- [18] Y.-P. An, L. Li, C.-Y. Xia, and H.-B. Zeng, *Phys. Rev. D* **109**, 106022 (2024).
- [19] Y. An, L. Li, and H. Zeng, (2024), [arXiv:2406.13965 \[cond-mat.quant-gas\]](https://arxiv.org/abs/2406.13965).
- [20] B. Goutéraux, F. Sottovia, and E. Mefford, *Physical Review D* **108**, L081903 (2023).
- [21] D. Areán, B. Goutéraux, E. Mefford, and F. Sottovia, *JHEP* **05**, 272 (2024), [arXiv:2312.08243 \[hep-th\]](https://arxiv.org/abs/2312.08243).
- [22] B. Goutéraux and E. Mefford, (2024), [arXiv:2407.07939 \[hep-th\]](https://arxiv.org/abs/2407.07939).
- [23] J. Armas and E. Have, *SciPost Phys.* **16**, 039 (2024), [arXiv:2304.09596 \[hep-th\]](https://arxiv.org/abs/2304.09596).
- [24] Y. An and L. Li, (2024), [arXiv:2409.08310 \[hep-th\]](https://arxiv.org/abs/2409.08310).
- [25] I. Amado, D. Areán, A. Jimenez-Alba, K. Landsteiner, L. Melgar, and I. S. Landea, *Journal of High Energy Physics* **2013**, 108 (2013).
- [26] Y. Hidaka, *Phys. Rev. Lett.* **110**, 091601 (2013).
- [27] P. Basu, J. He, A. Mukherjee, M. Rozali, and H.-H. Shieh, *JHEP* **10**, 092 (2010), [arXiv:1007.3480 \[hep-th\]](https://arxiv.org/abs/1007.3480).
- [28] R.-G. Cai, L. Li, L.-F. Li, and Y.-Q. Wang, *JHEP* **09**, 074 (2013), [arXiv:1307.2768 \[hep-th\]](https://arxiv.org/abs/1307.2768).
- [29] S. Lan, H. Liu, Y. Tian, and H. Zhang, [arXiv:2010.06232 \[hep-th\]](https://arxiv.org/abs/2010.06232).
- [30] S. Ishino, M. Tsubota, and H. Takeuchi, *Physical Review A* **88**, 063617 (2013).
- [31] S. Ishino, M. Tsubota, and H. Takeuchi, *Journal of Low Temperature Physics* **171**, 429 (2013).
- [32] P. Kuopanportti, S. Bandyopadhyay, A. Roy, and D. Angom, *Physical Review A* **100**, 033615 (2019).
- [33] J. Armas, J. Bhattacharya, A. Jain, and N. Kundu, *JHEP* **06**, 090 (2017), [arXiv:1612.08088 \[hep-th\]](https://arxiv.org/abs/1612.08088).
- [34] Z.-Q. Zhao, X.-K. Zhang, and Z.-Y. Nie, *Journal of High Energy Physics* **2023**, 23 (2023).